Supporting Information

Regulating Oxygen Vacancy Distribution in Perovskites via A-Site Cation Engineering for Water Oxidation

Zengyu Su[a], Jingpin Wu[a], Tao Song[b,c], Lele Duan[c], Peili Zhang[a], Licheng Sun[a,c*], Ke Fan[a,d*]

[a]*State Key Laboratory of Fine Chemicals, Institute of Artificial Photosynthesis, DUT-KTH Joint Education and Research Centre on Molecular Devices, Institute for Energy Science and Technology, Dalian University of Technology, 116024, Dalian, China*

[b]*Department of Chemistry, Southern University of Science and Technology, Shenzhen 518055, Guangdong, China*

[c]*Center of Artificial Photosynthesis for Solar Fuels and Department of Chemistry, School of Science, Westlake University, 310024 Hangzhou, P. R. China*

[d]*Interdisciplinary Institute of NMR and Molecular Sciences, School of Chemistry and Chemical Engineering, Wuhan University of Science and Technology, Wuhan 430081, P. R. China*

**Emails: sunlicheng@westlake.edu.cn;*

kefan@wust.edu.cn

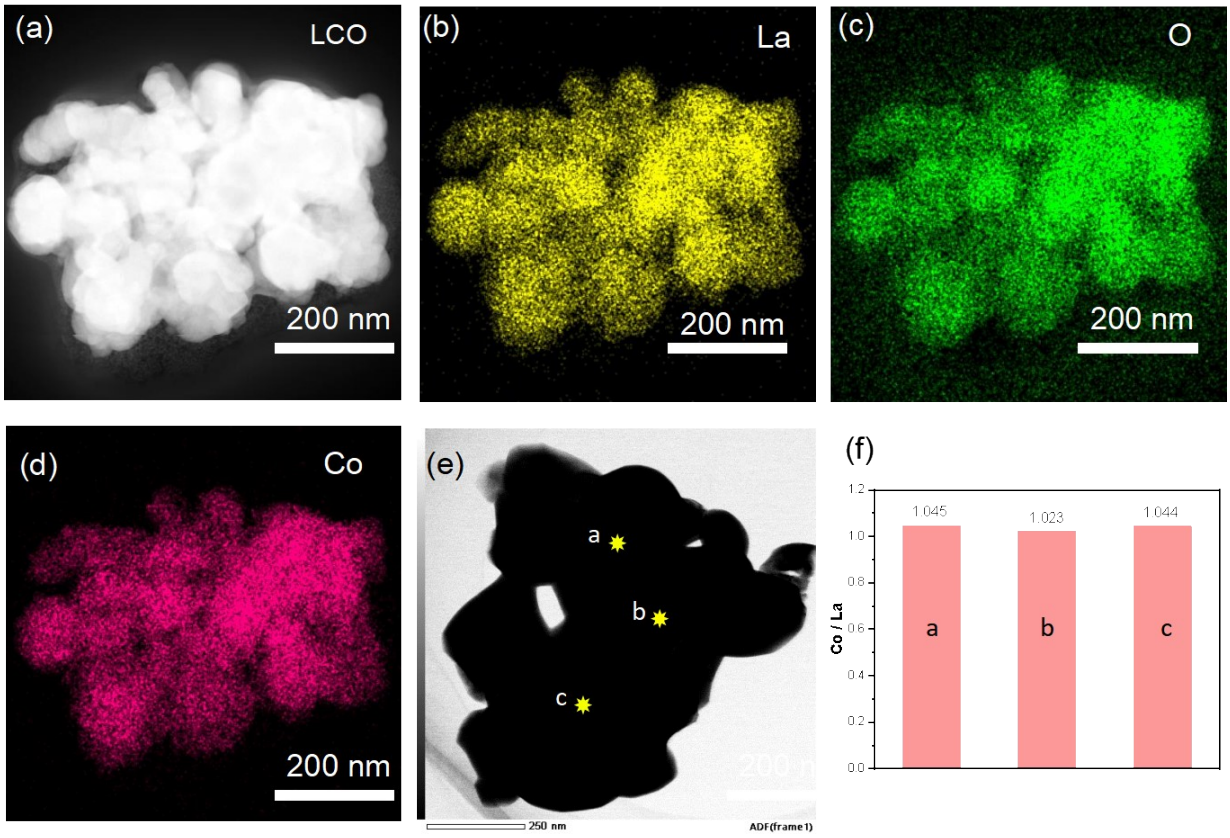

Fig. S1. (a-d) EDS mapping images of LCO. (e) Different locations used to determine the atomic ratios of A/B sites (indicated by yellow stars). (f) Atomic ratios of Co/La of LCO obtained from (e).

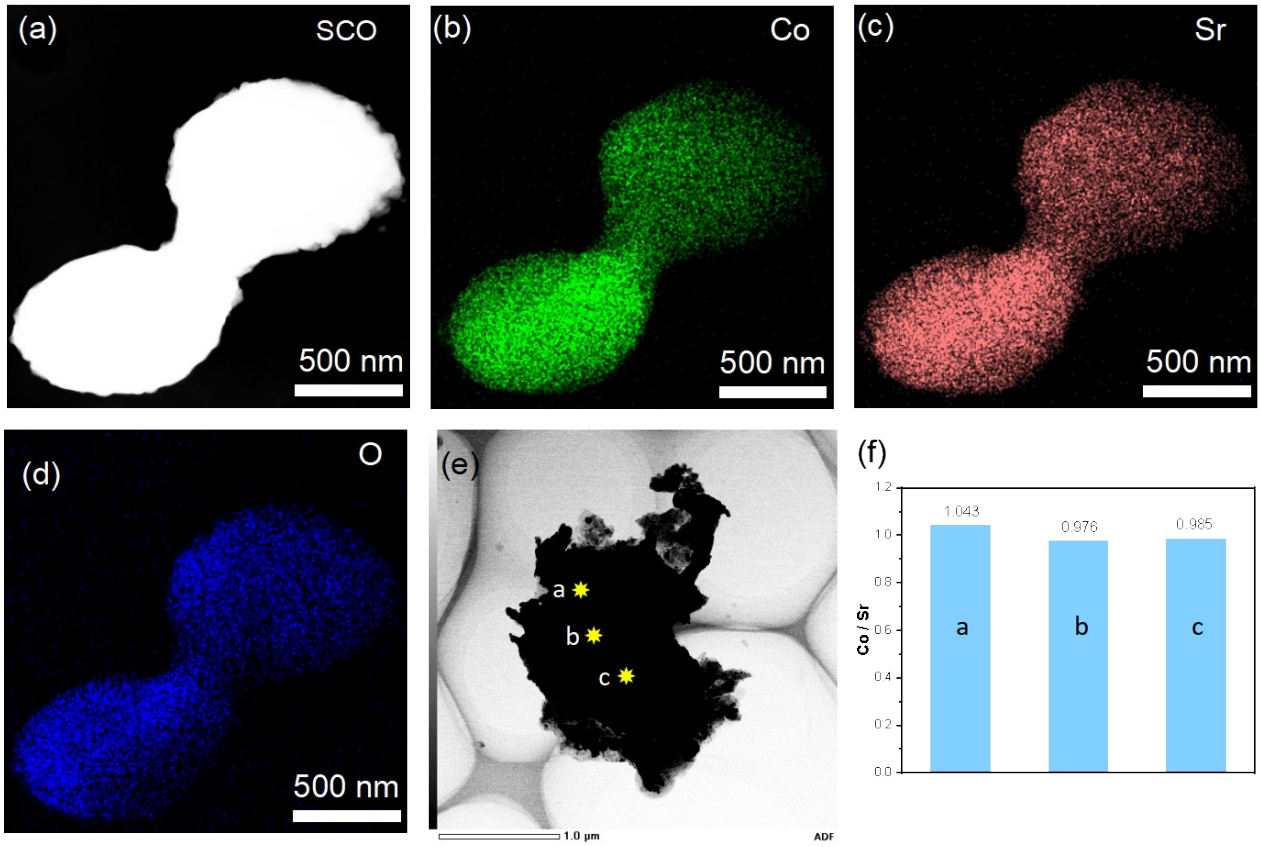

Fig. S2. (a-d) EDS mapping images of SCO. (e) Different locations used to determine the atomic ratios of A/B sites (indicated by yellow stars). (f) Atomic ratios of Co/Sr of LCO obtained from (e).

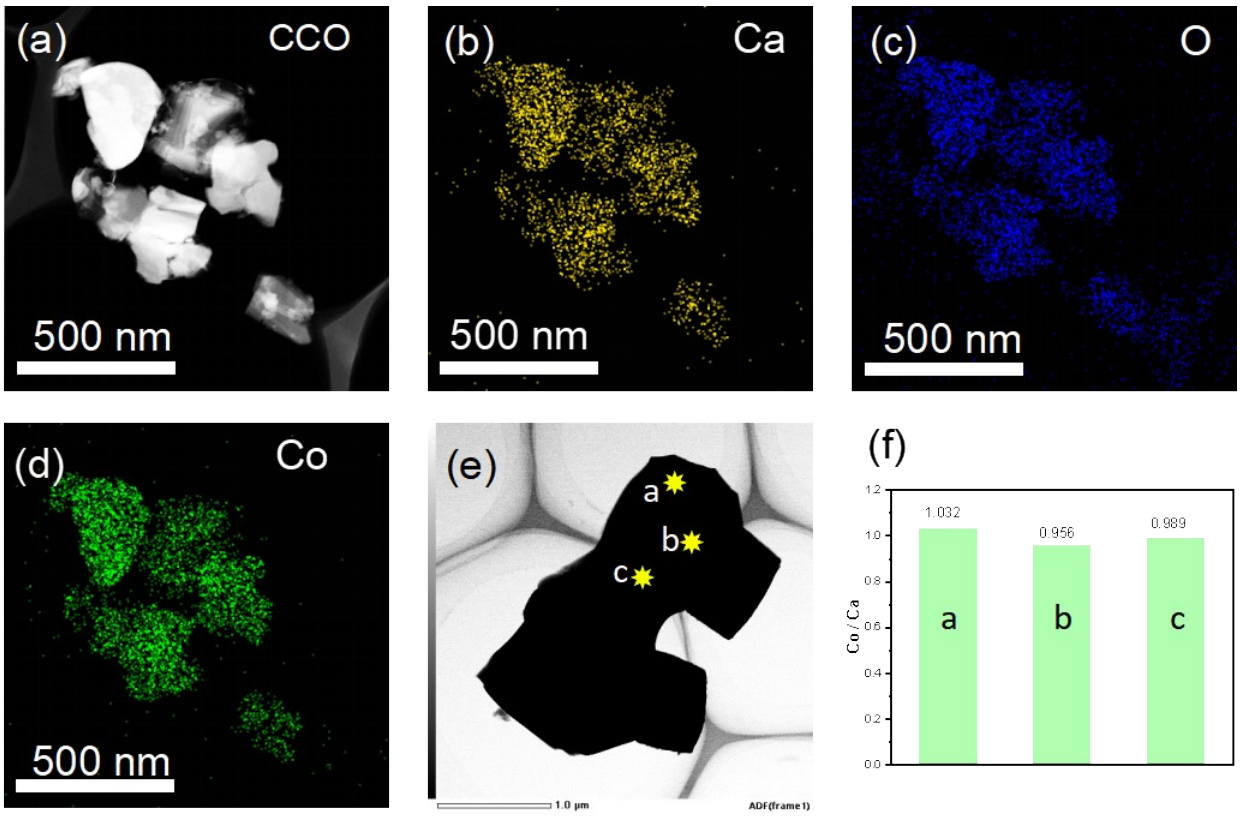

Fig. S3. (a-d) EDS mapping images of CCO. (e) Different locations used to determine the atomic ratios of A/B sites (indicated by yellow stars). (f) Atomic ratios of Co/Ca of LCO obtained from (e).

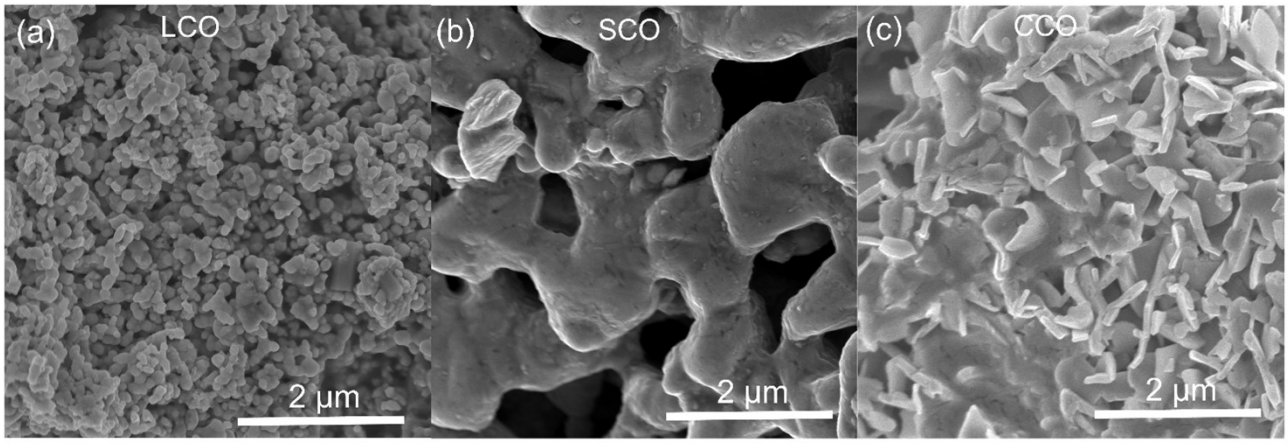

Fig. S4. SEM images of (a) LCO, (b) SCO, and (c) CCO.

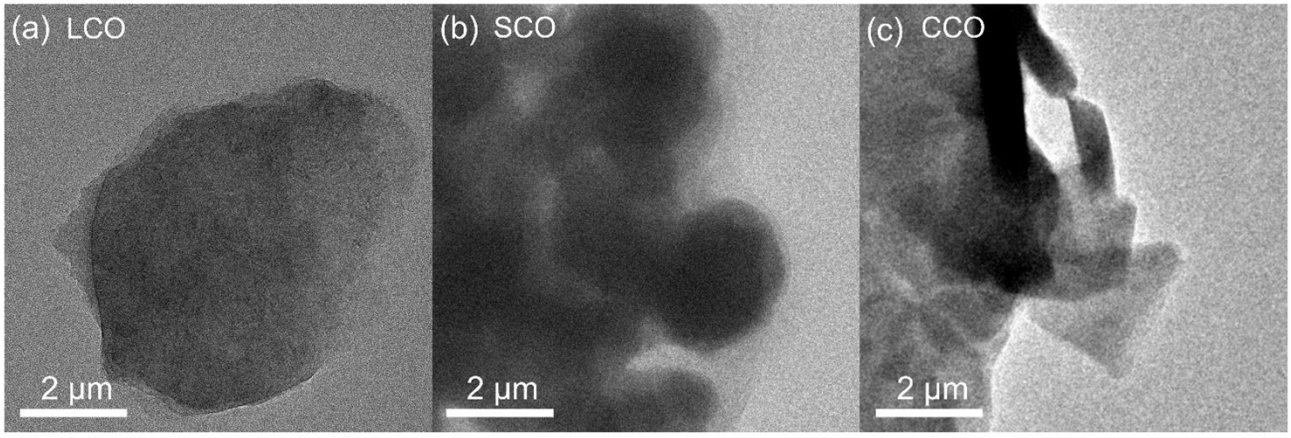

Fig. S5. TEM images of (a) LCO, (b) SCO, and (c) CCO.

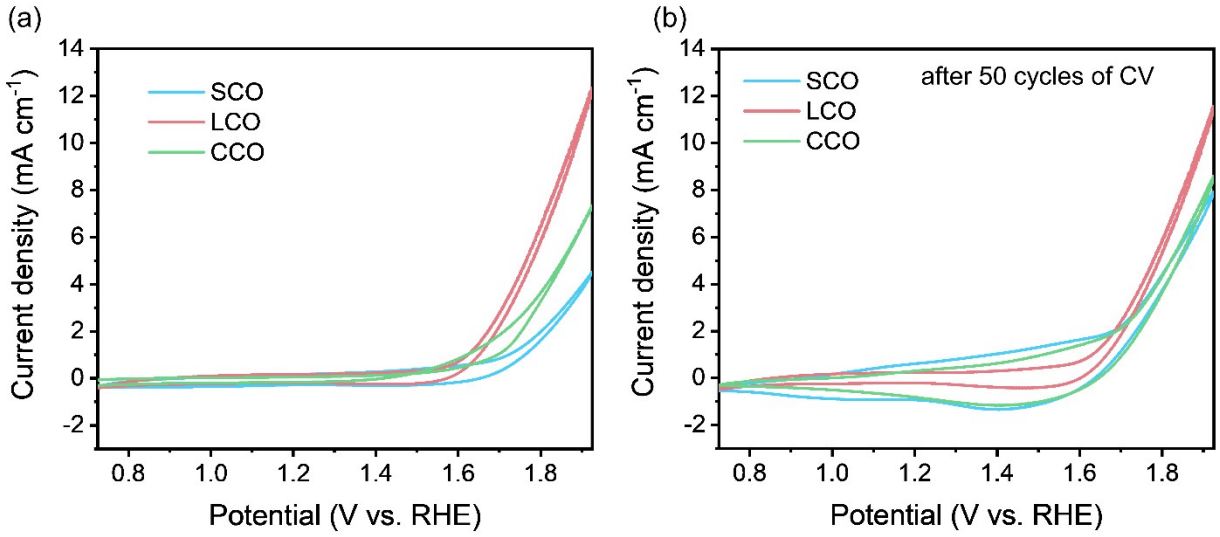

Fig. S6. (a) CV (0.72-1.92 V vs RHE) of the 1st and (b) 50th cycle of LCO, SCO and CCO.

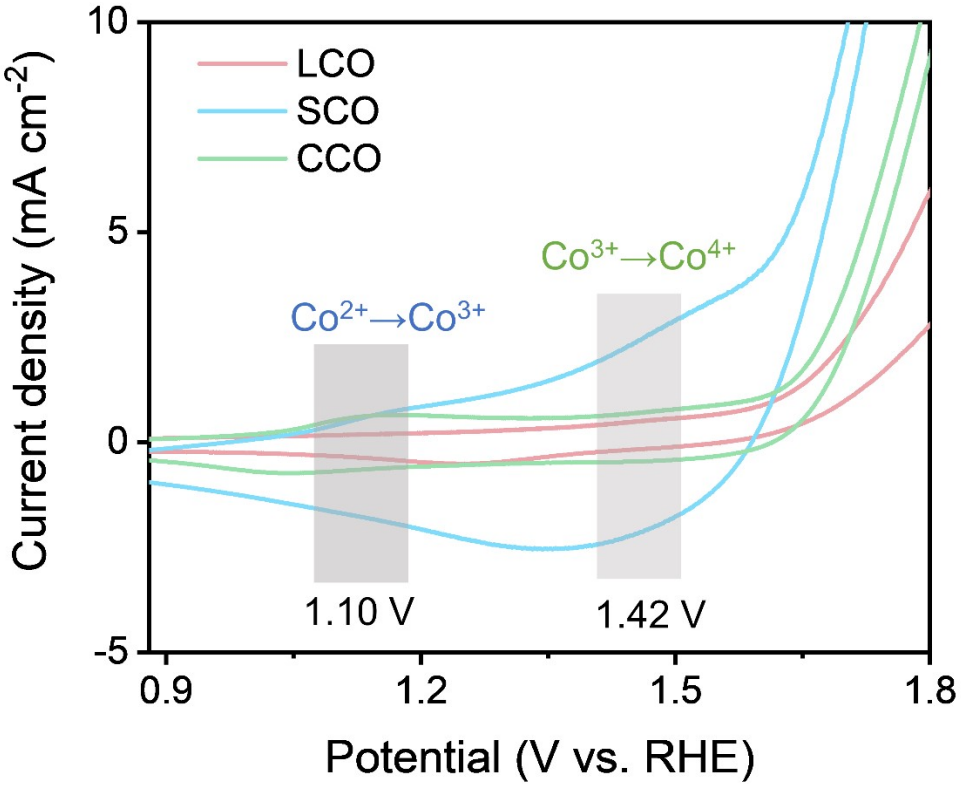

Fig. S7. Magnified view of CV curves.

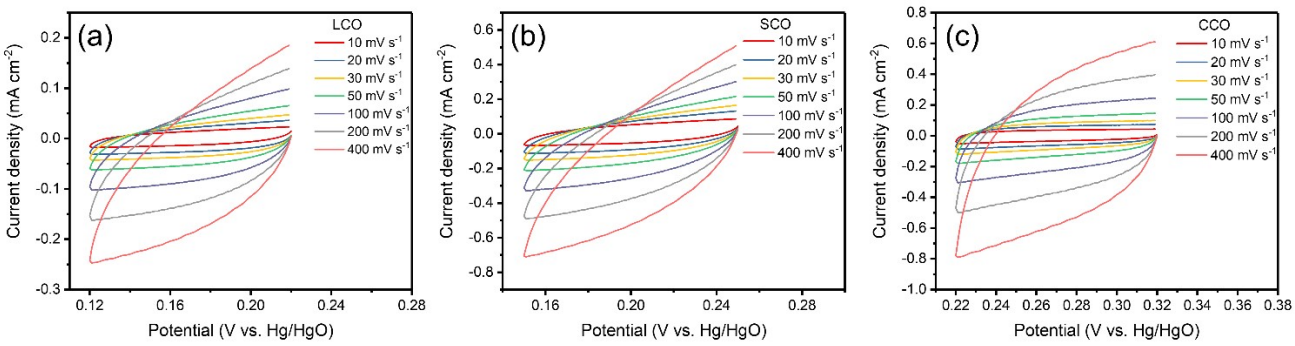

Fig. S8. CV curves in non-Faradic area at different scanning rate of (a) LCO, (b) SCO and (c) CCO.

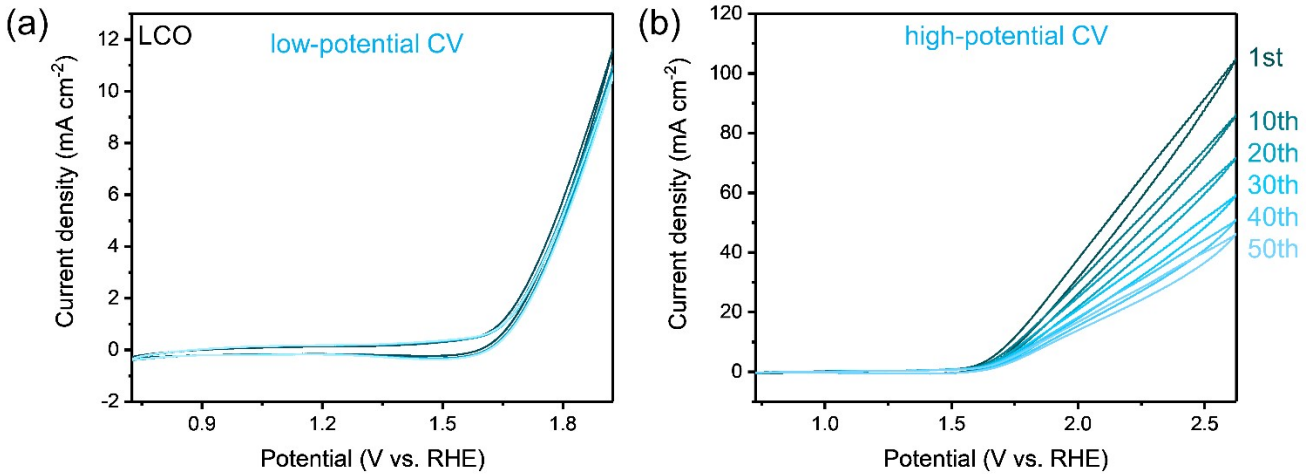

Fig. S9. CV curves (a) at low potentials and (b) high potentials of LCO.

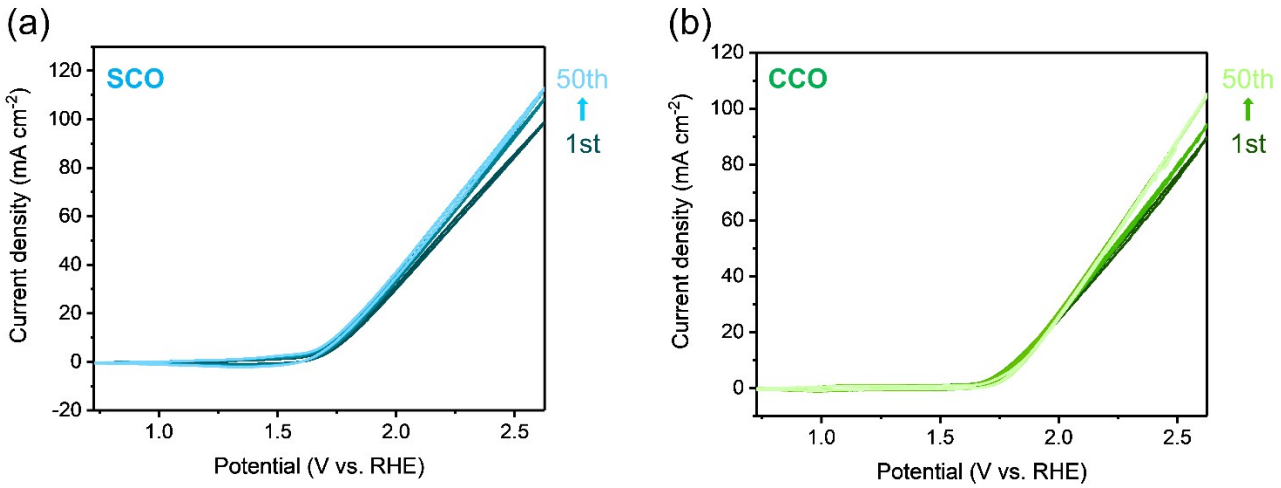

Fig. S10. CV curves at high potentials of (a) SCO and (b) CCO.

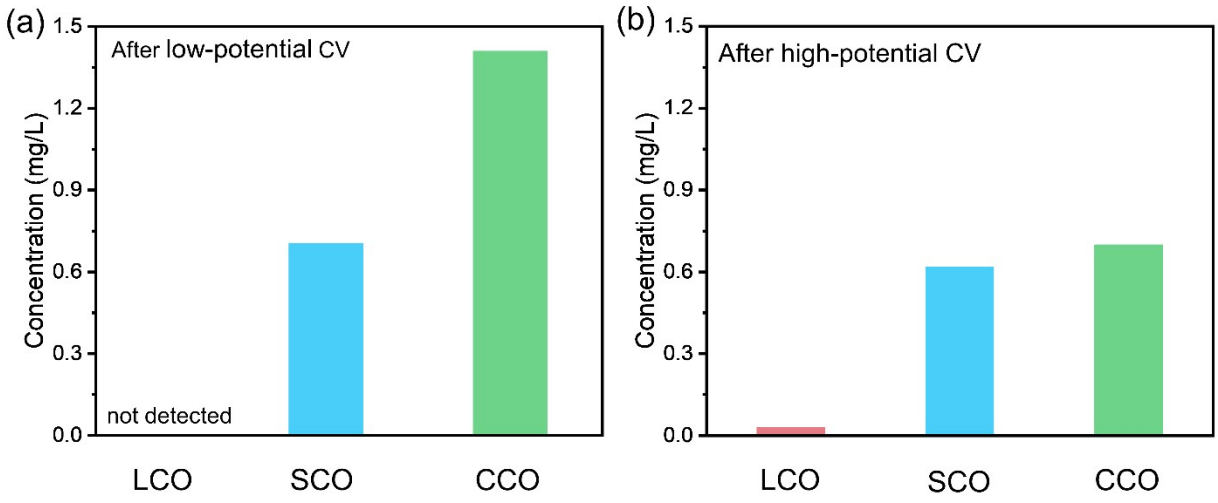

Fig. S11. ICP results after low- and high-potential CV.

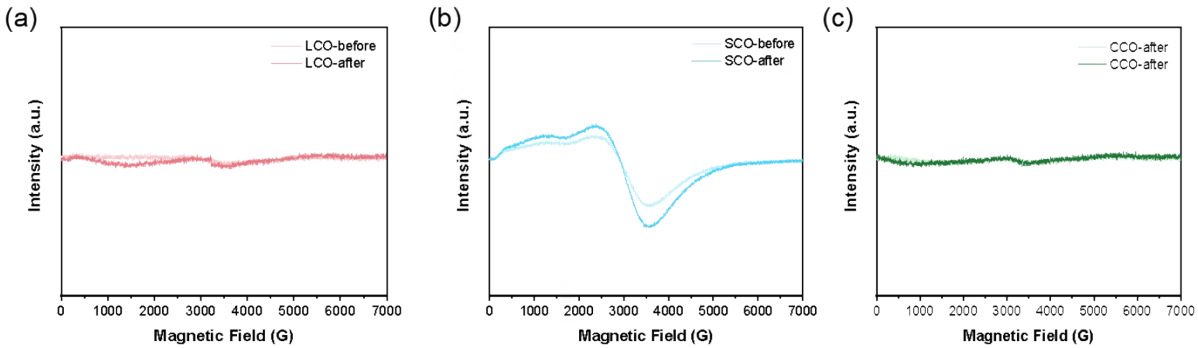

Fig. S12. EPR before and after catalytic reaction of (a) LCO, (b) SCO and (c) CCO.

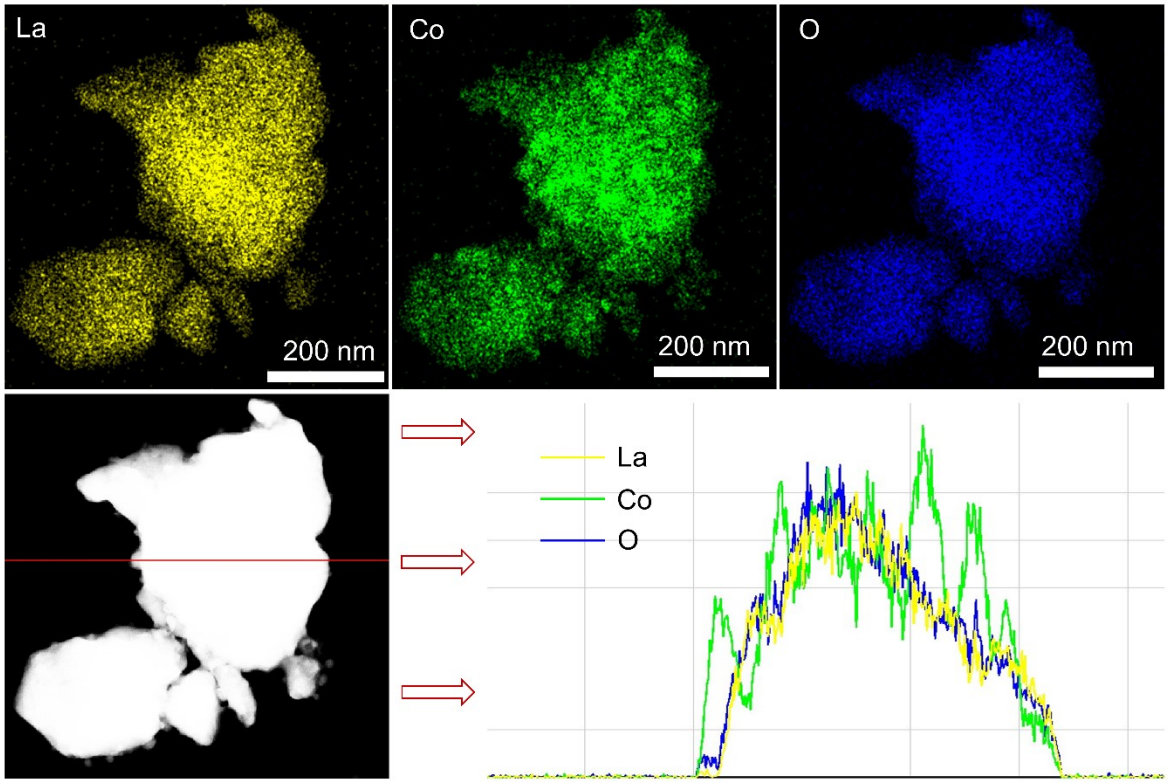

Fig. S13. EDS mapping and linear EDS scanning images of LCO after OER.

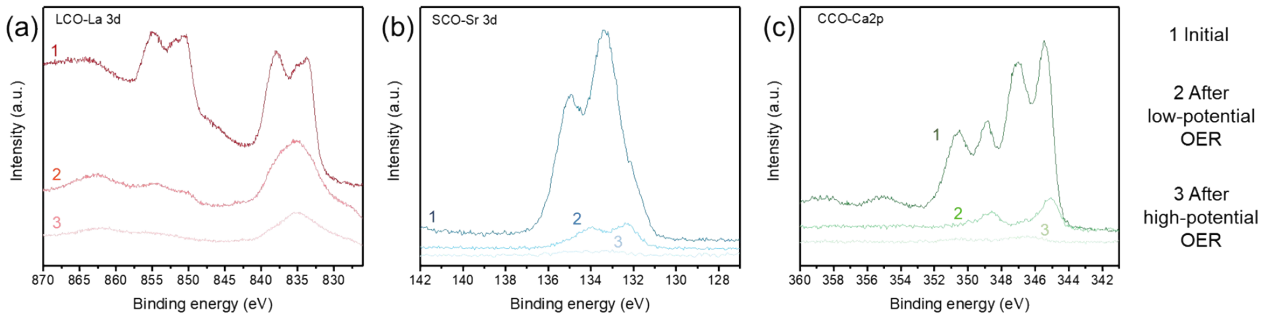

Fig. S14. (a) La 3d XPS of LCO, (b) Sr 3d XPS of SCO, (c) Ca 2p XPS of CCO.

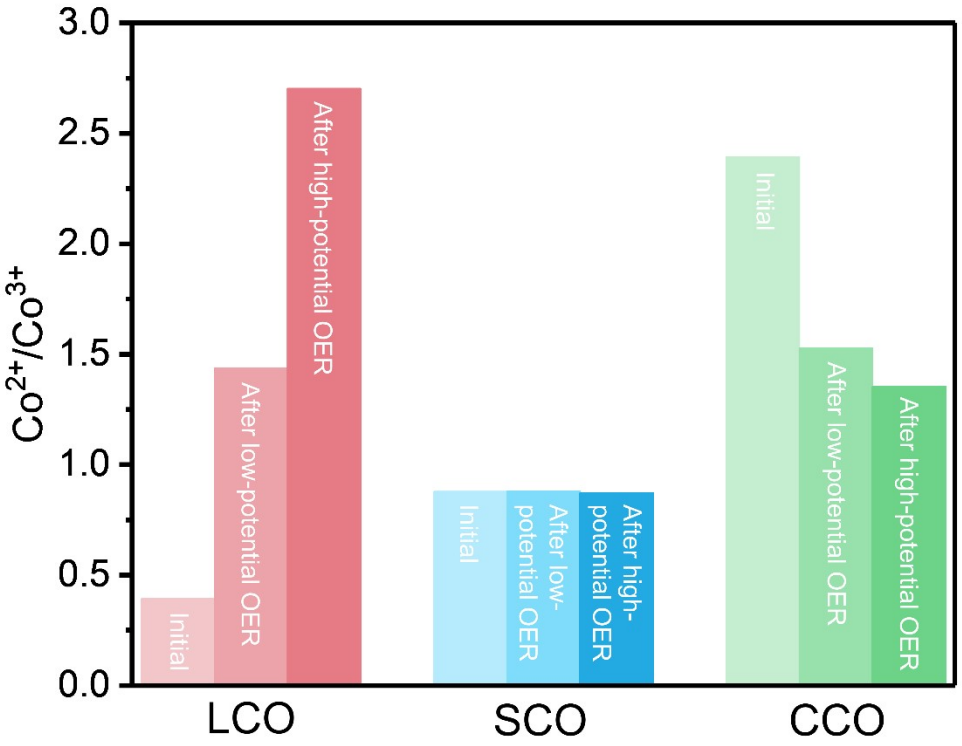

Fig. S15. Surface Co^{2+}/Co^{3+} of the initial, after low- and high-potential OER.

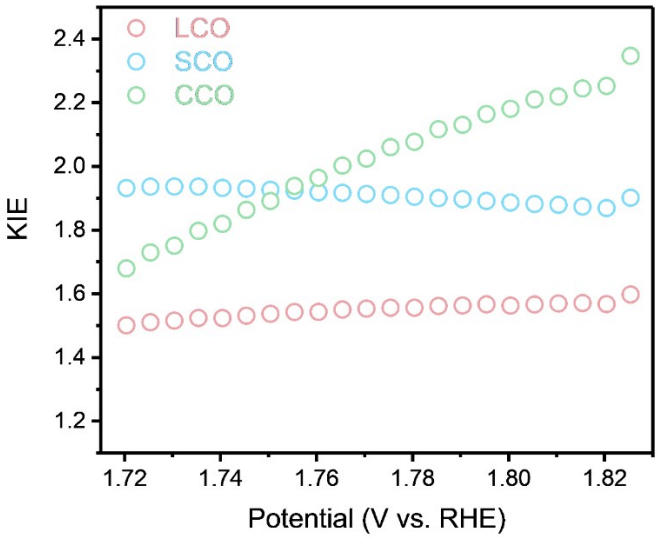

Fig. S16. KIE of LCO, SCO and CCO.

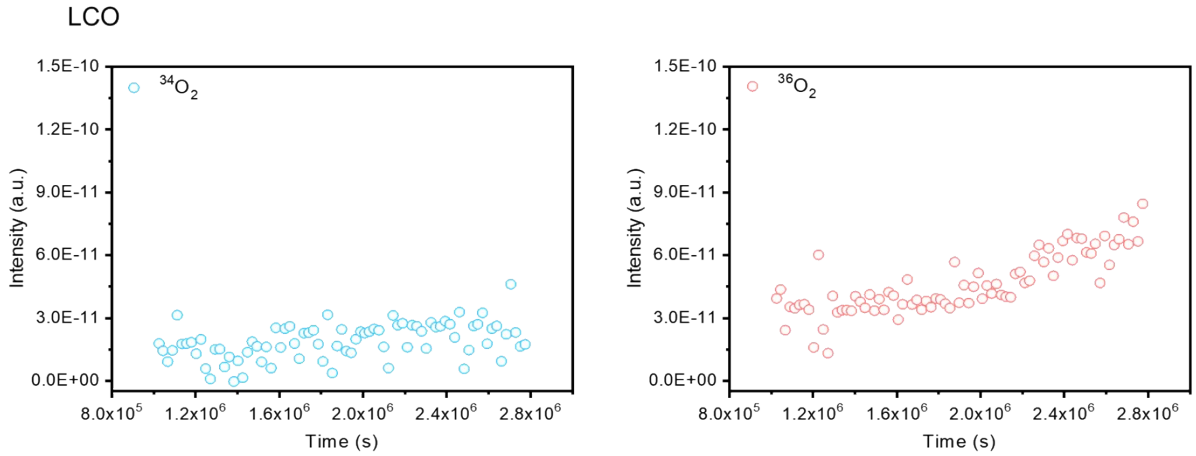

Fig. S17. OLEMS of LCO.

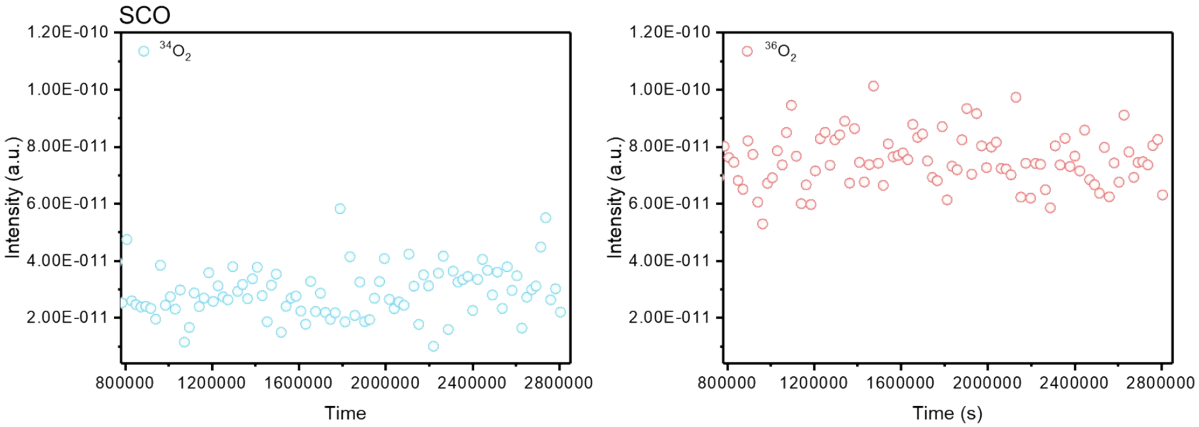

Fig. S18. OLEMS of SCO.

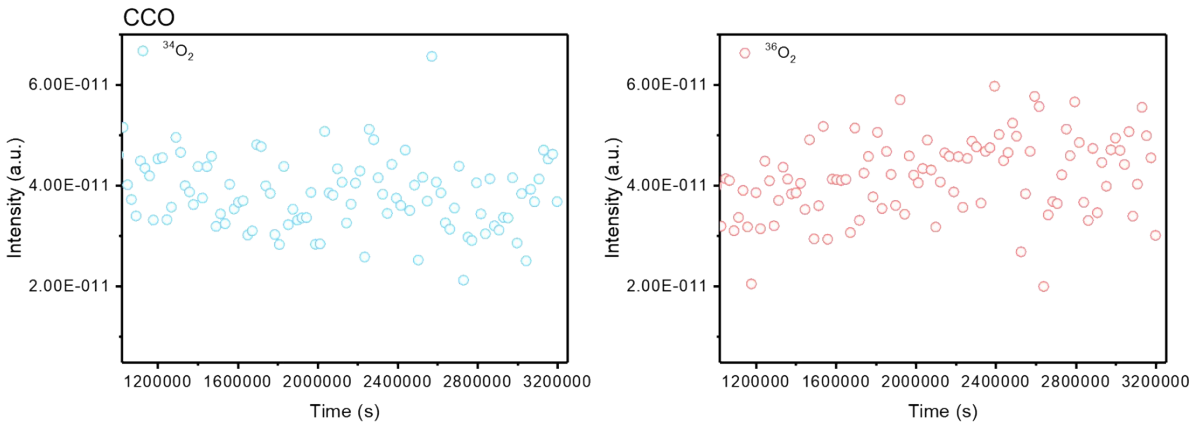

Fig. S19. OLEMS of CCO.